1

# Can Unsynchronized LEOs Provide 3D Orientation for a Ground Receiver?

Don-Roberts Emenonye, Harpreet S. Dhillon, and R. Michael Buehrer

Abstract-Large antenna arrays and reconfigurable intelligent surfaces (RIS) have been made available due to the use of higher frequency bands, and there is the possibility that these arrays can become disturbed. Hence, their orientation could change after deployment. Since low earth orbits (LEO) are being proposed to provide position, navigation, and timing services, and LEOs from different constellations could be unsynchronized in time and frequency and experience a high Doppler rate. "can unsynchronized LEOs provide 3D orientation for a ground receiver?" To answer this question, we introduce the Fisher information matrix (FIM) and use the FIM to quantify the available information needed for 3D orientation estimation utilizing signals received from LEOs during multiple transmission time slots across multiple receive antennas. We observe by analyzing the positive definitiveness of the FIM for the 3D orientation that irrespective of the presence or absence of both time and frequency offsets, the 3D orientation of the receiver can be estimated through the multiple TOA measurements received across the receive antennas from two LEO satellites during a single transmission time slot. We also observe by analyzing the positive definitiveness of the FIM for the 3D orientation that irrespective of the presence or absence of both time and frequency offsets, the 3D orientation of the receiver can be estimated through the multiple TOA measurements received across the receive antennas during two transmission time slots from a single LEO satellite.

# I. Introduction

The need for higher bandwidth has led to the exploration of higher frequency bands, which in turn enables the use of large antenna arrays [1] or reconfigurable intelligent surfaces (RIS) [2]. The size of these arrays causes the array orientation to become a non-negligible parameter that can be estimated. Moreover, especially in the case of RISs, the array can be disturbed, causing the orientation to change after placement. Hence, in this case of misorientation, the array orientation needs to be estimated and fed back to the network controller. A second case that highlights the importance of orientation is near-field communication [3]. Research on near-field communication has become prevalent because large antenna arrays can cause the Fraunhofer distance to be extended over several kilometers, causing near-field propagation effects rather than the usual far-field effects. In such propagation scenarios, there is more geometric information due to the spherical wavefronts as opposed to the planar wavefronts that are available during far-field propagation. This extra information can be utilized

D.-R. Emenonye, H. S. Dhillon, and R. M. Buehrer are with Wireless@VT, Bradley Department of Electrical and Computer Engineering, Virginia Tech, Blacksburg, VA, 24061, USA. Email: {donroberts, hdhillon, rbuehrer}@vt.edu. The support of the US National Science Foundation (Grants ECCS-2030215, CNS-1923807, and CNS-2107276) is gratefully acknowledged.

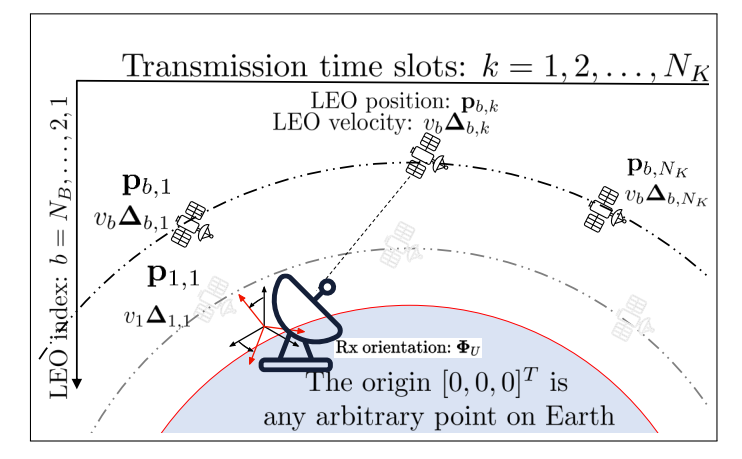


Figure 1. LEO-based localization systems with  $N_B$  LEOs transmitting during  $N_K$  transmission time slots to a receiver with  $N_U$  antennas.

through beam focusing [3], which in turn needs the array orientation. Since low earth orbit satellites (LEO) are several orders of magnitude closer to the Earth than the Global Navigation Satellite System (GNSS), they provide a position, navigation, and timing alternative in the inevitable scenarios where GNSS is unavailable (such as in deep urban canyons, under dense foliage, during unintentional interference, and intentional jamming) or untrustworthy (e.g., under malicious spoofing attacks), a research opportunity arises. Can we utilize the signals from LEOs that are unsynchronized in both time and frequency and received at a ground receiver to correct the receiver's orientation?

Research related to LEO-based positioning ranges from dedicated [4]–[10] to semi-opportunistic to opportunistic techniques [11], [12]. Authors in [5] assume that the reference signal is known and provides a Fisher information matrix (FIM) study of the 3D position of a receiver. In [6], the proximity of LEOs in comparison to GNSS inspires a study of broadband LEOs for navigation. The authors in [7] present an economic investigation of utilizing LEOs for localization. The design of reference signals for LEO positioning systems is studied in [8], [9]. The authors in [10] investigates using positioning information to improve communication systems. Although research is ongoing and extensive, quantifying the utility of the signals from multiple LEOs during multiple transmission time slots across multiple receive antennas for the estimation of the 3D orientation of a receiver is an area that has not been studied. Hence, in this work, we use the FIM to quantify the available information needed for 3D orientation estimation in signals received from LEOs during multiple

transmission time slots across multiple receive antennas.

#### II. SYSTEM MODEL

We consider  $N_B$  single antenna LEO satellites, each communicating with a receiver with  $N_U$  antennas, through transmissions in  $N_K$  different time slots. The transmission slots are spaced by  $\Delta_t$ . At the  $k^{\text{th}}$  transmission time slot, the  $N_B$  LEO satellites are located at  $p_{b,k}, b \in \{1, 2, \dots, N_B\}$  and  $k \in$  $\{1, 2, \cdots, N_K\}$ . The points,  $p_{b,k}$ , are described with respect to a global origin. During the  $k^{\text{th}}$  time slot, the receiver has an arbitrary but known geometry with its centroid located at  $p_{U,k}$ .

During the  $k^{th}$  time slot, the point,  $s_u$ , describes the  $u^{th}$ receive antenna with respect to the centroid while the point,  $p_{u,k}$ , describes the position of this element with respect to the global origin as  $p_{u,k} = p_{U,k} + s_u$ . The point,  $s_u$ , can be written as  $s_u = Q_U \tilde{s}_u$  where  $\tilde{s}_u$  aligns with the global reference axis and  $Q_U = Q(\alpha_U, \psi_U, \varphi_U)$  defines a 3D rotation matrix [13]. The orientation angles of the receiver are vectorized as  $\mathbf{\Phi}_U = [\alpha_U, \psi_U, \varphi_U]^T$ . The centroid of the receiver at point,  $p_{U,k}$  with respect to the  $b^{th}$ LEO can be written as  $p_{U,k} = p_{b,k} + d_{bU,k} \Delta_{bU,k}$  where  $d_{bU,k}$  is the distance from point  $p_{b,k}$  to point  $p_{U,k}$  and  $\Delta_{bU,k}$  is the corresponding unit direction vector  $\Delta_{bU,k}$  =  $[\cos \phi_{bU,k} \sin \theta_{bU,k}, \sin \phi_{bU,k} \sin \theta_{bU,k}, \cos \theta_{bU,k}]^{\mathrm{T}}$ . During the  $k^{\text{th}}$  transmission time slot, the angles  $\phi_{bU,k}$  and  $\theta_{bU,k}$  represent the angle in the azimuth and elevation from the  $b^{th}$  LEO satellite to the receiver.

# A. Transmit and Receive Processing

The  $N_B$  LEO satellites transmit in  $N_K$  different time slots, each of equal durations. At time t, during the k<sup>th</sup> time slot, the bth LEO satellite uses quadrature modulation and transmits the following signal to the receiver  $x_{b,k}[t] = s_{b,k}[t] \exp(j2\pi f_c t)$ , where  $s_{b,k}[t]$  is the complex signal envelope of the signal transmitted by the  $b^{th}$  LEO satellite during the  $k^{th}$  time slot, and  $f_c = c/\lambda$  is the operating frequency of LEO satellites. The speed of light is c, and  $\lambda$  is the operating wavelength. The channel model from the LEO satellites to the receiver consists only of the LOS paths. With this channel model and the transmit signal, the signal at the  $u^{th}$  receive antenna during the  $k^{th}$  time slot is

$$y_{u,k}[t] = \sum_{b=1}^{N_B} y_{bu,k}[t],$$

$$= \sum_{b=1}^{N_b} \beta_{bu,k} \sqrt{2} \Re \left\{ s_{b,k}[t_{obu,k}] \exp(j(2\pi f_{ob,k} t_{obu,k})) \right\}$$

$$+ n_{u,k}[t],$$

$$= \mu_{u,k}[t] + n_{u,k}[t],$$
(1)

where  $\mu_{u,k}[t]$  and  $n_{u,k}[t] \sim \mathcal{CN}(0, N_0)$  are the noise-free part (useful part) of the signal and the Fourier transformed thermal noise local to the receiver's antenna array, respectively. Also,  $\beta_{bu,k}$  is the channel gain from the  $b^{th}$  LEO satellite observed at the  $u^{\rm th}$  receive antenna during the  $k^{\rm th}$  time slot,  $f_{ob,k}=$  $f_c(1-\nu_{b,k})+\epsilon_b$  is the observed frequency at receiver with respect to the  $b^{\text{th}}$  LEO satellite, and  $t_{obu,k} = t - \tau_{bu,k} + \delta_b$ is the effective time duration. In the observed frequency,  $\nu_{b,k}$ is the Doppler with respect to the  $b^{\text{th}}$  LEO satellite, and  $\epsilon_b$ is the frequency offset measured with respect to the  $b^{th}$  LEO satellite.

In the effective time duration,  $\delta_b$  is the time offset at the receiver measured with respect to the bth LEO satellite, and the delay from the  $u^{th}$  receive antenna to the  $b^{th}$  LEO satellite during the  $k^{\text{th}}$  time slot is  $\tau_{bu,k} \triangleq \frac{\|\mathbf{p}_{u,k} - \mathbf{p}_{b,k}\|}{c}$ .

**Remark 1.** The offset,  $\delta_b$ , captures the unknown time offset as well as the unknown ionospheric and tropospheric delay concerning the b<sup>th</sup> LEO satellite.

Here, the position of the  $b^{th}$  LEO satellite and the  $u^{\text{th}}$  receive antenna during the  $k^{\text{th}}$  time slot is  $\mathbf{p}_{b,k} = \mathbf{p}_{b,o} + \tilde{\mathbf{p}}_{b,k}$ , and  $\mathbf{p}_{u,k} = \mathbf{p}_{u,o} + \tilde{\mathbf{p}}_{U,k}$ , Here,  $\mathbf{p}_{b,o}$  and  $\mathbf{p}_{u,o}$  are the reference points of the  $b^{\text{th}}$  LEO satellite and the  $u^{\text{th}}$  receive antenna, respectively. The distance travelled by the bth LEO satellite and the  $u^{th}$  receive antenna are  $\tilde{\mathbf{p}}_{b,k}$  and  $\tilde{\mathbf{p}}_{u,k}$ , respectively. These traveled distances can be described as  $\tilde{\mathbf{p}}_{b,k} = (k-1)\Delta_t v_b \mathbf{\Delta}_{b,k}$ , and  $\tilde{\mathbf{p}}_{U,k} = (k-1)\Delta_t v_U \mathbf{\Delta}_{U,k}$ , respectively. Here,  $v_b$  and  $v_U$  are speeds of the  $b^{th}$  LEO satellite and receiver, respectively. The associated directions are defined as  $\Delta_{b,k} = [\cos \phi_{b,k} \sin \theta_{b,k}, \sin \phi_{b,k} \sin \theta_{b,k}, \cos \theta_{b,k}]^{\mathrm{T}}$ and  $\Delta_{U,k} = [\cos \phi_{U,k} \sin \theta_{U,k}, \sin \phi_{U,k} \sin \theta_{U,k}, \cos \theta_{U,k}]^{\mathrm{T}},$ respectively. Now, the velocity of the bth LEO satellite and the velocity of the receiver are  $v_{b,k} = v_b \Delta_{b,k}$ and  $v_{U,k} = v_U \Delta_{U,k}$ , respectively. Hence, the Doppler observed by the receiver from the bth LEO satellite is  $u_{b,k} = \boldsymbol{\Delta}_{bU,k}^{\mathrm{T}}(\boldsymbol{v}_{b,k} - \boldsymbol{v}_{U,k}).$ 

# B. Properties of the Received Signal

In this section, we discuss the properties that are observable in the signal at the receiver across all receive antennas and during all the transmission slots. To accomplish this, we consider the Fourier transform of the baseband signal that is transmitted by the  $b^{\text{th}}$  LEO satellite at time t during the  $k^{\text{th}}$  time slot  $S_{b,k}[f] \triangleq \frac{1}{\sqrt{2\pi}} \int_{-\infty}^{\infty} s_{b,k}[t] \exp\left(-j2\pi ft\right) \ dt$ . This Fourier transform is called the spectral density.

1) Effective Baseband Bandwidth: This can be viewed as the average of the squared of all frequencies normalized by the area occupied by the spectral density,  $S_{b,k}$ . Mathematically, the effective baseband bandwidth is  $\alpha_{1b,k} \triangleq$ 

$$\left(\frac{\int_{-\infty}^{\infty} f^2 |S_{b,k}[f]|^2 df}{\int_{-\infty}^{\infty} |S_{b,k}[f]|^2 df}\right)^{\frac{1}{2}}.$$

2) Received Signal-to-Noise Ratio: The SNR is the ratio of the power of the signal across its occupied frequencies to the noise spectral density. Mathematically, the SNR is  $SNR \triangleq SNR$ 

$$\frac{8\pi^{2}|\beta_{bu,k}|^{2}}{N_{0}} \int_{-\infty}^{\infty} |S_{b,k}[f]|^{2} df$$

 $\frac{8\pi^2|\beta_{bu,k}|^2}{N_0} \int_{-\infty}^{\infty} |S_{b,k}[f]|^2 df.$  The mathematical description of the available information useful for 3D orientation estimation is written in terms of these received signal properties.

# III. AVAILABLE INFORMATION IN THE RECEIVED SIGNAL

In this section, we define the parameters, both geometric channel parameters and nuisance parameters.

# A. Error Bounds on Parameters

The analysis in this section is based on the received signal given by (1), which is obtained from  $N_B$  LEO satellites on  $N_U$  receive antennas during  $N_K$  distinct time slots of T durations each. The parameters observable in the signal received by a receiver from the  $b^{th}$  LEO satellite on its  $N_U$ receive antenna during the  $N_K$  different time slots are subsequently presented. The delays observed across the  $N_U$  receive antennas during the  $k^{\rm th}$  time slots are presented in vector form  $au_{b,k} \triangleq [ au_{b1,k}, au_{b2,k}, \cdots, au_{bN_U,k}]^{\mathrm{T}}$ , then the delays across the  $N_U$  receive antennas during all  $N_K$  time slots are also vectorized as follows  $\boldsymbol{\tau}_b \triangleq \left[\boldsymbol{\tau}_{b,1}^{\mathrm{T}}, \boldsymbol{\tau}_{b,2}^{\mathrm{T}}, \cdots, \boldsymbol{\tau}_{b,N_K}^{\mathrm{T}}\right]^{\mathrm{T}}$ . The Doppler observed with respect to the  $b^{\mathrm{th}}$  LEO satellite across all the  $N_K$  transmission time slots is  $\nu_b \triangleq [\nu_{b,1}, \nu_{b,2}, \cdots, \nu_{b,N_K}]^{\mathrm{T}}$ . Next, the channel gain across the  $N_U$  receive antennas during the  $k^{\text{th}}$  time slots are presented in vector form  $\boldsymbol{\beta}_{b,k} \triangleq$  $[\beta_{b1,k},\beta_{b2,k},\cdots,\beta_{bN_U,k}]^{\mathrm{T}}$ , then the delays across the  $N_U$  receive antennas during all  $N_K$  time slots are also vectorized as follows  $\beta_b \triangleq \left[\beta_{b,1}^{\mathrm{T}}, \beta_{b,2}^{\mathrm{T}}, \cdots, \beta_{b,N_K}^{\mathrm{T}}\right]^{\mathrm{T}}$ . Note that if there is no beam split, the channel gain remains constant across all antennas and is simply  $\beta_b \triangleq \left[\beta_{b,1}, \beta_{b,2}, \cdots, \beta_{b,N_K}\right]^{\mathrm{T}}$ . Moreover, if the channel gain is constant across all time slots, we can further represent the bth LEO transmission by the scalar,  $\beta_b$ . Finally, with these vectorized forms, the total parameters observable in the signals received at a receiver from the  $b^{th}$  LEO satellite on its  $N_U$  receive antenna during the  $N_K$  different time slots are vectorized as follows  $\boldsymbol{\eta}_b^{\mathrm{T}} \triangleq \begin{bmatrix} \boldsymbol{\tau}_b^{\mathrm{T}}, \boldsymbol{\nu}_b^{\mathrm{T}}, \boldsymbol{\beta}_b^{\mathrm{T}}, \delta_b, \epsilon_b \end{bmatrix}^{\mathrm{T}}$ . All signals observable from all  $N_B$  LEO satellites across  $N_U$  receive antennas during the  $N_K$  different time slots are vectorized as  $\boldsymbol{\eta}^T \triangleq$  $\left[m{\eta}_1^{\mathrm{T}},m{\eta}_2^{\mathrm{T}},\cdots,m{\eta}_{N_B}^{\mathrm{T}}
ight]^{\mathrm{T}}$  . After specifying the parameters that are present in the signals received from the LEO satellites - considering the time slots and receive antennas, we present the mathematical preliminaries needed for further discussions.

## B. Mathematical Preliminaries

Although we have specified the parameters in the signals received in a LEO-based localization system, we still have to investigate the estimation accuracy achievable when estimating these parameters. Moreover, it's unclear whether all the parameters presented are separately observable and can contribute to a localization framework. One way of answering these two questions is by using the FIM.

**Definition 1.** The general FIM for a parameter vector,  $\eta$ , defined as  $\mathbf{J}_{y;\eta} = \mathbf{F}_{y;\eta}(y;\eta;\eta,\eta)$  is the summation of the FIM obtained from the likelihood due to the observations defined as  $\mathbf{J}_{y|oldsymbol{\eta}} = F_y(y|oldsymbol{\eta};oldsymbol{\eta},oldsymbol{\eta})$  and the FIM from a priori information about the parameter vector defined as  $\mathbf{J}_{\eta} = F_{\eta}(\eta; \eta, \eta)$ . In mathematical terms, we have  $\mathbf{J}_{y;\eta} \triangleq -\mathbb{E}_{y;\eta} \left[ \frac{\partial^2 \ln \chi(y;\eta)}{\partial \eta \partial \eta^{\mathrm{T}}} \right]$ 

 $= -\mathbb{E}_{\boldsymbol{y}} \left[ \frac{\partial^2 \ln \chi(\boldsymbol{y}|\boldsymbol{\eta})}{\partial \boldsymbol{\eta} \partial \boldsymbol{\eta}^{\mathrm{T}}} \right] - \mathbb{E}_{\boldsymbol{\eta}} \left[ \frac{\partial^2 \ln \chi(\boldsymbol{\eta})}{\partial \boldsymbol{\eta} \partial \boldsymbol{\eta}^{\mathrm{T}}} \right]$   $= \mathbf{J}_{\boldsymbol{y}|\boldsymbol{\eta}} + \mathbf{J}_{\boldsymbol{\eta}}, \text{ where } \chi(\boldsymbol{y};\boldsymbol{\eta}) \text{ denotes the probability density}$ function (PDF) of y and  $\eta$ .

**Definition 2.** Given a parameter vector,  $\boldsymbol{\eta} \triangleq \left[\boldsymbol{\eta}_1^{\mathrm{T}}, \boldsymbol{\eta}_2^{\mathrm{T}}\right]^{\mathrm{T}}$ , where  $\eta_1$  is the parameter of interest, the resultant FIM has the structure  $\mathbf{J}_{\boldsymbol{y};\boldsymbol{\eta}} = \begin{bmatrix} \mathbf{J}_{\boldsymbol{y};\boldsymbol{\eta}_1}\mathbf{J}_{\boldsymbol{y};\boldsymbol{\eta}_1,\boldsymbol{\eta}_2} \\ \mathbf{J}_{\boldsymbol{y};\boldsymbol{\eta}_1,\boldsymbol{\eta}_2}^T\mathbf{J}_{\boldsymbol{y};\boldsymbol{\eta}_2} \end{bmatrix}$ , where  $\boldsymbol{\eta} \in \mathbb{R}^N, \boldsymbol{\eta}_1 \in \mathbb{R}^n, \mathbf{J}_{\boldsymbol{y};\boldsymbol{\eta}_1} \in \mathbb{R}^{n \times n}, \mathbf{J}_{\boldsymbol{y};\boldsymbol{\eta}_1,\boldsymbol{\eta}_2} \in \mathbb{R}^{n \times (N-n)}$ , and  $\mathbf{J}_{\boldsymbol{y};\boldsymbol{\eta}_2} \in \mathbb{R}^{(N-n) \times (N-n)}$  with n < N, and the EFIM [14] of parameter  $\boldsymbol{\eta}_1$  is given by  $\mathbf{J}_{\boldsymbol{y};\boldsymbol{\eta}_1}^e = \mathbf{J}_{\boldsymbol{y};\boldsymbol{\eta}_1} - \mathbf{J}_{\boldsymbol{y};\boldsymbol{\eta}_1}^{nu} = \mathbf{J}_{\boldsymbol{y};\boldsymbol{\eta}_1}$  $\mathbf{J}_{oldsymbol{y};oldsymbol{\eta}_1} - \mathbf{J}_{oldsymbol{y};oldsymbol{\eta}_1,oldsymbol{\eta}_2} \mathbf{J}_{oldsymbol{y};oldsymbol{\eta}_1,oldsymbol{\eta}_2}^{-1} \mathbf{J}_{oldsymbol{y};oldsymbol{\eta}_1,oldsymbol{\eta}_2}^{\mathrm{T}}.$ 

# C. Fisher Information Matrix for Channel Parameters

In the definitions of the FIM and EFIM given in the previous section, the expression of the likelihood of the received signal conditioned on the parameter vector is required. This likelihood for the received signal conditioned on the parameter vector is defined considering the  $N_B$  LEO satellites,  $N_U$ receive antennas, and the  $N_K$  time slots, and is presented next.

$$\chi(\boldsymbol{y}[t]|\boldsymbol{\eta}) \propto \prod_{b=1}^{N_B} \prod_{u=1}^{N_U} \prod_{k=1}^{N_K} \exp\left\{ \frac{2}{N_0} \int_0^T \Re\left\{ \mu_{bu,k}^{\mathrm{H}}[t] y_{bu,k}[t] \right\} dt - \frac{1}{N_0} \int_0^T |\mu_{bu,k}[t]|^2 dt \right\}.$$
(2)

Subsequently, this FIM due to the observations from the  $N_B$  LEO satellite, received across the  $N_U$  antennas, and during the  $N_K$  distinct time slots can be computed with the likelihood function (2) and Definition 1, and it results in the diagonal matrix  $\mathbf{J}_{m{y}|m{\eta}} = F_{m{y}}(m{y}|m{\eta};m{\eta},m{\eta}) =$  $\operatorname{diag}\left\{ oldsymbol{F_y}(oldsymbol{y}|oldsymbol{\eta};oldsymbol{\eta}_1,oldsymbol{\eta}_1),\dots,oldsymbol{F_y}(oldsymbol{y}|oldsymbol{\eta};oldsymbol{\eta}_{N_B},oldsymbol{\eta}_{N_B}) 
ight\}.$ entries in FIM due to the observations of the received signals from bth LEO satellite can be obtained through the simplified expression.  $F_y(y|\eta;\eta_b,\eta_b)$  $\frac{1}{N_0} \sum_{u,k}^{N_U N_K} \Re \left\{ \int \nabla_{\eta_b} \mu_{bu,k}[t] \nabla_{\eta_b} \mu_{bu,k}^{\mathrm{H}}[t] \ dt \right\}$ . The non-zero elements in the FIM are presented next. Considering the bth LEO satellite, the FIM focusing on the delays at the  $u^{th}$  receive antenna during the  $k^{th}$  time slot is  $F_{\mathbf{y}}(\mathbf{y}|\boldsymbol{\eta}; \tau_{bu,k}, \tau_{bu,k}) = -F_{\mathbf{y}}(\mathbf{y}|\boldsymbol{\eta}; \tau_{bu,k}, \delta_b) = \underset{bu,k}{\operatorname{SNR}}\omega_{b,k}.$ 

where 
$$\omega_{b,k} = \left[\alpha_{1b,k}^2 + f_{ob,k}^2\right]$$
.

The FIM focusing on the Doppler observed with respect to the  $b^{th}$  LEO satellite at the receiver during the  $k^{th}$  time slot is presented next. The FIM of the Doppler observed with respect to the  $b^{\rm th}$  LEO satellite at the receiver during the  $k^{\rm th}$  time slot is  $F_y(y|\eta;\nu_{b,k},\nu_{b,k})=0.5* \underset{bu,k}{\mathrm{SNR}} f_c^2 t_{obu,k}^2$ . The FIM of the Doppler observed with respect to the  $b^{th}$  LEO satellite and

the corresponding frequency offset during the  $k^{th}$  time slot is  $\begin{aligned} \pmb{F_y(y|\eta;\nu_{b,k},\epsilon_b)} &= -0.5* \underset{bu,k}{\mathrm{SNR}} f_c t_{obu,k}^2. \end{aligned}$  The FIM of the channel gain in the FIM due to the

observations of the received signals from bth LEO satellite to the  $u^{\text{th}}$  receive antenna during the  $k^{\text{th}}$  time slot is  $F_{\boldsymbol{y}}(\boldsymbol{y}|\boldsymbol{\eta};\beta_{bu,k},\beta_{bu,k}) = \frac{1}{4\pi^2|\beta_{bu,k}|^2} \underset{bu,k}{\text{SNR}}.$ 

The FIM focusing on the time offset at the  $u^{th}$  receive antenna during the  $k^{th}$  time slot with respect to the  $b^{th}$  LEO satellite is presented next. The FIM of the time offset in the FIM due to the observations of the received signals from  $b^{th}$ 

With the assumption that the parameters from different LEO satellites are independent.

LEO satellite to the  $u^{\rm th}$  receive antenna during the  $k^{\rm th}$  time slot is

$$F_{\mathbf{y}}(\mathbf{y}|\boldsymbol{\eta};\delta_b,\delta_b) = F_{\mathbf{y}}(\mathbf{y}|\boldsymbol{\eta};\tau_{bu,k},\tau_{bu,k}) = -F_{\mathbf{y}}(\mathbf{y}|\boldsymbol{\eta};\delta_b,\tau_{bu,k}).$$

The FIM focusing on the frequency offset at the  $u^{\rm th}$  receive antenna during the  $k^{\rm th}$  time slot with respect to the  $b^{\rm th}$  LEO satellite is presented next. The FIM of the frequency offset in the FIM due to the observations of the received signals from  $b^{\rm th}$  LEO satellite to the  $u^{\rm th}$  receive antenna during the  $k^{\rm th}$  time slot is  $F_{\boldsymbol{y}}(\boldsymbol{y}|\boldsymbol{\eta};\epsilon_b,\epsilon_b) = 0.5* \underset{bu,k}{\mathrm{SNR}} t_{obu,k}^2.$ 

The FIM of the channel parameters, based on the observations of the received signals, is used to derive the FIM for the receiver's 3D orientation in the next section.

# IV. FISHER INFORMATION MATRIX FOR LOCATION PARAMETERS

In the previous section, we highlighted the useful and nuisance parameters present in the signals received from the  $N_B$  LEO satellites across the  $N_U$  receive antennas during  $N_K$  different time slots. Subsequently, we derived the information about these parameters present in the received signals and presented the structure of these parameters. In this section, we use the FIM for channel parameters to derive the FIM for the location parameters and highlight the FIM structure. This FIM for the location parameters will help us determine how feasible it is to find the 3D orientation of a receiver with the signals received from LEO satellites.

To proceed, we define the location parameters  $\kappa = [\Phi_U, \zeta_1, \zeta_2, \cdots, \zeta_{N_B}]$ , where  $\zeta_b = [\beta_b^{\rm T}, \delta_b, \epsilon_b]^{\rm T}$ , and our goal is to derive the FIM of the entire location parameter vector, or different combinations of parameters, under different levels of uncertainty about the channel parameters. The FIM for the location parameters,  $\mathbf{J}_{y|\kappa}$  can be obtained from the FIM for the channel parameters,  $\mathbf{J}_{y|\eta}$ , using the bijective transformation  $\mathbf{J}_{y|\kappa} \triangleq \Upsilon_{\kappa} \mathbf{J}_{y|\eta} \Upsilon_{\kappa}^{\rm T}$ , where  $\Upsilon_{\kappa}$  represents derivatives of the non-linear relationship between the geometric channel parameters,  $\eta$ , and the location parameters [15]. The elements in the bijective transformation matrix  $\Upsilon_{\kappa}$  are given in Appendix A. With no *a priori* information about the location parameters  $\kappa$ ,  $\mathbf{J}_{y;\kappa} = \mathbf{J}_{y|\kappa}$ . The EFIM taking  $\kappa_1 = \Phi_U$  as the parameter of interest and  $\kappa_2 = [\zeta_1, \zeta_2, \cdots, \zeta_{N_B}]$  as the nuisance parameters is now derived.

# A. Elements in $J_{y;\kappa_1}$

The elements in  $J_{y;\kappa_1}$  are presented through the following Lemmas. This FIM corresponds to the available information of the location parameters  $\kappa_1$  when the nuisance parameters are known.

**Lemma 1.** The FIM of the 3D orientation of the receiver is 
$$\mathbf{F}_{y}(\mathbf{y}|\boldsymbol{\eta}; \boldsymbol{\Phi}_{U}, \boldsymbol{\Phi}_{U}) = \sum_{b,k,u} \underset{bu,k}{\mathrm{SNR}} \left[ \omega_{b,k} \nabla_{\boldsymbol{\Phi}_{U}} \tau_{bu,k} \nabla_{\boldsymbol{\Phi}_{U}}^{\mathrm{T}} \tau_{bu,k} \right].$$

# B. Elements in $\mathbf{J}_{\boldsymbol{y};\boldsymbol{\kappa}_1}^{nu}$

The elements in  $\mathbf{J}_{y;\kappa_1}^{nu}$  are presented in this section. These elements represent the loss of information about  $\kappa_1$  due to uncertainty in the nuisance parameters  $\kappa_2$ .

**Lemma 2.** The loss of information about 3D orientation of the receiver due to uncertainty in the nuisance parameters  $\kappa_2$  is  $G_y(y|\eta; \Phi_U, \Phi_U) = \sum_b \sum_{k,uk',u'} \sup_{bu,k} \sup_{bu',k'} \nabla_{\Phi_U} \tau_{bu,k} \nabla_{\Phi_U}^T \tau_{bu',k'} \omega_{b,k} \times \omega_{b,k'} \left(\sum_{u,k} \sup_{bu,k} \sum_{bu,k} \sum$ 

The elements in the EFIM for the location parameters,  $\mathbf{J}^{\mathrm{e}}_{y;\kappa_1}$  are obtained by appropriately combining the Lemmas in Section IV-A and the Lemmas in Section IV-B. The EFIM for the location parameters is  $\mathbf{J}^{\mathrm{e}}_{y;\kappa_1} = \mathbf{J}_{y;\kappa_1} - \mathbf{J}^{nu}_{y;\kappa_1} = \mathbf{J}_{y;\kappa_1} - \mathbf{J}^{nu}_{y;\kappa_1} + \mathbf{J}^{-1}_{y;\kappa_1,\kappa_2} \mathbf{J}^{-1}_{y;\kappa_1,\kappa_2} \mathbf{J}^{-1}_{y;\kappa_1,\kappa_2}$ . Here, we consider available information for estimating the 3D orientation. This information is specified by the EFIM of the 3D orientation of the receiver and is given by (3).

# V. NUMERICAL RESULTS

This section presents simulation results that describe the available information in signals received from LEO satellites during multiple transmission time slots on receivers with multiple antennas. We start by showing the minimum infrastructure needed to estimate the 3D orientation. More specifically, we present the minimum number of LEO satellites, time slots, and receive antennas that contribute to 3D orientation estimation. We also present the Cramer Rao bound (CRB) for 3D orientation as a function of the spacing between transmission time slots.

We use the following simulation parameters. The SNR is assumed constant across the transmission time slots and receive antennas, and the following set of SNR values is considered:  $\{40~\mathrm{dB}, 20~\mathrm{dB}, 0~\mathrm{dB}, -20~\mathrm{dB}\}$ . The x,y, and z components of the position of the LEO satellites are randomly chosen, but LEO satellites are approximately 2000 km from the receiver. The x,y, and z components of the velocity of the LEO satellites are randomly chosen and change every transmission time slot to depict acceleration, but the LEO satellites have a speed of 8000 m/s. The receiver's position's x,y, and z components are randomly chosen, but the receiver is approximately 30 m from the origin. The x,y, and z components of the receiver's velocity are randomly chosen and remain constant to depict constant velocity, but the receiver has a speed of 25 m/s. The effective baseband bandwidth,  $\alpha_{1b,k}$ , is 100 MHz.

# A. 3D Orientation Estimation

Here, we investigate the minimal number of time slots, LEO satellites, and receive antennas that produce a positive definite FIM for the 3D orientation of the receiver, which is defined by (3).

- 1)  $N_K=1$ ,  $N_B=2$ , and  $N_U>1$ : Irrespective of the presence or absence of both time and frequency offsets, the 3D orientation of the receiver can be estimated through the multiple TOA measurements received across the receive antennas from both LEO satellites.
- 2)  $N_K=2$ ,  $N_B=1$ , and  $N_U>1$ : Irrespective of the presence or absence of both time and frequency offsets, the 3D orientation of the receiver can be estimated through the multiple TOA measurements received across the receive antennas during both time slots from the LEO satellite.

$$\mathbf{J}_{\boldsymbol{y};\boldsymbol{\Phi}_{U}}^{e} = \left[\mathbf{J}_{\boldsymbol{y};\boldsymbol{\kappa}_{1}}^{e}\right] = F_{y}(\boldsymbol{y}|\boldsymbol{\eta};\boldsymbol{\Phi}_{U},\boldsymbol{\Phi}_{U}) - G_{y}(\boldsymbol{y}|\boldsymbol{\eta};\boldsymbol{\Phi}_{U},\boldsymbol{\Phi}_{U}) \\
= \sum_{b,k,u} \frac{\mathrm{SNR}}{\mathrm{suk}} \left[\omega_{b,k} \nabla_{\boldsymbol{\Phi}_{U}} \tau_{bu,k} \nabla_{\boldsymbol{\Phi}_{U}}^{\mathrm{T}} \tau_{bu,k}\right] - \sum_{b} \sum_{k,uk',u'} \frac{\mathrm{SNR} \, \mathrm{SNR}}{\mathrm{suk},k} \nabla_{\boldsymbol{\Phi}_{U}} \tau_{bu,k} \nabla_{\boldsymbol{\Phi}_{U}}^{\mathrm{T}} \tau_{bu',k'} \omega_{b,k} \omega_{b,k'} \left(\sum_{u,k} \frac{\mathrm{SNR} \, \omega_{b,k}}{\mathrm{suk},k}\right)^{-1}.$$
(3)

#### B. Simulation results

Here, we present simulation results for the CRLB when estimating  $\Phi_U$  with  $N_K=2$ ,  $N_B=1$ , and  $N_U>1$ . In Fig. 2, we notice an improvement in orientation error due to an increase in the length of the time interval between the transmission time slots is more clearly seen. This reduction in orientation error is slow from 25 ms to 100 ms but is drastic above 100 ms. This improvement in orientation error is due to the speed of the LEO satellites. The speed of satellites means that the same satellite can act as multiple anchors in different time slots while still achieving good geometric dilution of precision.

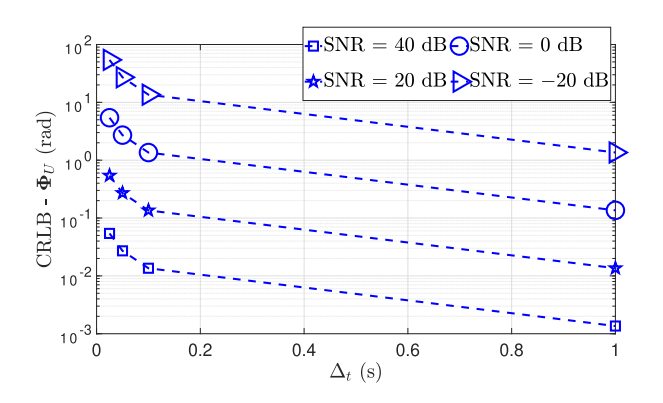


Figure 2. CRLB for  $\Phi_U$  with  $f_c=1$  GHz and  $N_U=4$ : focuses on  $\Delta_t$  values from  $\Delta_t=25$  ms to  $\Delta_t=1$  s.

## VI. CONCLUSION

In this paper, we have asked, "can unsynchronized LEOs provide 3D orientation for a ground receiver?" To answer this question, we introduced the FIM. We used the FIM to quantify the information needed for 3D orientation present in signals received from LEOs during multiple transmission time slots across multiple receive antennas. We observed by analyzing the positive definitiveness of the FIM of the 3D orientation that irrespective of the presence or absence of both time and frequency offsets, the 3D orientation of the receiver can be estimated through the multiple TOA measurements received across the receive antennas from two LEO satellites during a single transmission time slot. We also observed by analyzing the positive definitiveness of the FIM of the 3D orientation that irrespective of the presence or absence of both time and frequency offsets, the 3D orientation of the receiver can be estimated through the multiple TOA measurements received across the receive antennas during two transmission time slots from a single LEO satellite.

#### **APPENDIX**

# A. Entries in transformation matrix

The derivative of the delay from the  $u^{\text{th}}$  receive antenna to the  $b^{\text{th}}$  LEO satellite during the  $k^{\text{th}}$  time slot with respect to  $\alpha_U$  is  $\nabla_{\alpha_U} \tau_{bu,k} \triangleq \frac{\Delta_{bu,k}^{\text{T}} \nabla_{\alpha_U} Q_U \tilde{s}_u}{c}$ . The derivative of the delay from the  $u^{\text{th}}$  receive antenna to the  $b^{\text{th}}$  LEO satellite during the  $k^{\text{th}}$  time slot with respect to  $\psi_U$  is  $\nabla_{\psi_U} \tau_{bu,k} \triangleq \frac{\Delta_{bu,k}^{\text{T}} \nabla_{\psi_U} Q_U \tilde{s}_u}{c}$ . The derivative of the delay from the  $u^{\text{th}}$  receive antenna to the  $b^{\text{th}}$  LEO satellite during the  $k^{\text{th}}$  time slot with respect to  $\varphi_U$  is  $\nabla_{\varphi_U} \tau_{bu,k} \triangleq \frac{\Delta_{bu,k}^{\text{T}} \nabla_{\varphi_U} Q_U \tilde{s}_u}{c}$ . The derivative of the delay from the  $u^{\text{th}}$  receive antenna to the  $b^{\text{th}}$  LEO satellite during the  $k^{\text{th}}$  time slot with respect to  $\Phi_U$  is

$$abla_{\Phi_U} au_{bu,k} riangleq rac{\Delta_{bu,k}^{\mathrm{T}} 
abla_{lpha_U} Q_U ilde{s}_u}{\Delta_{bu,k}^{\mathrm{T}} 
abla_{\psi_U} Q_U ilde{s}_u} \, 
ight].$$

# REFERENCES

- G. Bacci, L. Sanguinetti, and E. Björnson, "Spherical wavefronts improve mu-mimo spectral efficiency when using electrically large arrays," *IEEE Wireless Commun. Lett.*, Apr. 2023.
- [2] D.-R. Emenonye, H. S. Dhillon, and R. M. Buehrer, "RIS-aided localization under position and orientation offsets in the near and far field," *IEEE Trans. on Wireless Commun.*, vol. 22, no. 12, pp. 9327–9345, Dec. 2023
- [3] H. Zhang, N. Shlezinger, F. Guidi, D. Dardari, M. F. Imani, and Y. C. Eldar, "Beam focusing for near-field multiuser mimo communications," *IEEE Transactions on Wireless Communications*, vol. 21, no. 9, pp. 7476–7490, Sep. 2022.
- [4] H. K. Dureppagari, C. Saha, H. S. Dhillon, and R. M. Buehrer, "NTN-based 6G localization: Vision, role of LEOs, and open problems," *IEEE Wireless Communications*, vol. 30, no. 6, pp. 44–51, Dec. 2023.
- [5] J. Kang, P. E. N, J. Lee, H. Wymeersch, and S. Kim, "Fundamental performance bounds for carrier phase positioning in LEO-PNT systems," in *Proc.*, *IEEE Intl. Conf. on Acoustics, Speech, and Sig. Proc. (ICASSP)*, 2024, pp. 13496–13500.
- [6] T. Reid, A. Neish, T. Walter, and P. Enge, "Broadband LEO constellations for navigation," *Navigation*, vol. 65, Jun. 2018.
  [7] P. A. Iannucci and T. E. Humphreys, "Economical fused LEO GNSS,"
- [7] P. A. Iannucci and T. E. Humphreys, "Economical fused LEO GNSS," in *Proc.*, *IEEE/ION Position, Location and Navigation Symposium* (*PLANS*), 2020, pp. 426–443.
- [8] A. Nardin, F. Dovis, and J. A. Fraire, "Empowering the tracking performance of LEO-based positioning by means of meta-signals," *IEEE J. of Radio Frequency Identification*, vol. 5, no. 3, pp. 244–253, Sep. 2021
- [9] D. Egea-Roca, J. López-Salcedo, G. Seco-Granados, and E. Falletti, "Performance analysis of a multi-slope chirp spread spectrum signal for pnt in a LEO constellation," in proc., Satellite Navigation Technology Workshop (NAVITEC), 2022, pp. 1–9.
- [10] L. You, X. Qiang, Y. Zhu, F. Jiang, C. G. Tsinos, W. Wang, H. Wymeer-sch, X. Gao, and B. Ottersten, "Integrated communications and localization for massive MIMO LEO satellite systems," *IEEE Trans. on Wireless Commun.*, to appear.
- Z. M. Kassas, J. Morales, and J. J. Khalife, "New-age satellite-based navigation STAN: Simultaneous tracking and navigation with LEO satellite signals," 2019. [Online]. Available: https://api.semanticscholar.org/CorpusID:214300844
   M. Neinavaie, J. Khalife, and Z. M. Kassas, "Acquisition, doppler
- [12] M. Neinavaie, J. Khalife, and Z. M. Kassas, "Acquisition, doppler tracking, and positioning with starlink LEO satellites: First results," *IEEE Trans. on Aerospace and Electronic Systems*, vol. 58, no. 3, pp. 2606–2610, Apr. 2022.
- [13] S. M. LaValle, *Planning Algorithms*. Cambridge University Press, 2006.
- [14] Y. Shen and M. Z. Win, "Fundamental limits of wideband localization — part I: A general framework," *IEEE Trans. on Info. Theory*, vol. 56, no. 10, pp. 4956–4980, Oct. 2010.
- [15] S. M. Kay, Fundamentals of Statistical Signal Processing: Estimation Theory. Prentice-Hall, Inc., 1993.